Available online at www.sciencedirect.com

ScienceDirect

Procedia Engineering 66 (2013) 300 – 312

Procedia Engineering

www.elsevier.com/locate/procedia

5th Fatigue Design Conference, Fatigue Design 2013

Fatigue life model for 7050 chromic anodized aluminium alloy

Michel Chaussumier [a]*, Catherine Mabru [a], Rémy Chieragatti [a], Majid Shahzad [a]

Université de Toulouse; INSA, UPS, EMAC, ISAE; ICA (Institut Clément Ader), 10 Av. Edouard Belin, 31055 Toulouse Cedex 4, France

Abstract

Fatigue investigation on 7050-T7651 chromic acid anodized aluminium alloy has been realized in order to develop a fatigue life predictive model which includes the different experimental aspects of fatigue cracking. In particular, it has been observed that, for this alloy and the sub-mentioned anodizing process conditions, degreasing process used after machining had no influence on fatigue resistance; the essential of the important fatigue resistance decrease was due to pickling process, leading to production of numerous pits which were found to be crack initiation sites; then anodizing process was responsible for a supplementary increase of fatigue resistance decrease. Failure surfaces observations have shown that these pits were responsible for cracks and numerous crack coalescence phenomena have been pointed out.

The fatigue life predictive model presented in this paper is based on Suraratchaï's model, developed at ICA-Toulouse, which is built on the stress concentration effect of machining surface roughness: here pickling pits are considered as stress concentrators from which cracks could occur if stress intensity factor is high enough; considering the very low size of pickling pits, half size of middle recrystallized grain size, this implies the introduction in the model of short cracks considerations such as short crack stress intensity factor range threshold and short crack growth rate law. Coalescence conditions are also introduced. Calculation are conducted from a 3D finite elements built from experimental topographic measurements which allow the determination of stress concentration coefficients induced by machining surface roughness and the presence of the pits. Anodized surface are rebuilt from pickled surface in order to overturn the lack of accuracy during topographic surface measurements. Predictive results fit very well with experimental results whatever the surface state.

Keywords: pickling, anodizing, fracture mechanic, short crack growth rate law, life prediction, aluminium alloys,

* Corresponding author. Tel.: +33561339291; fax: +33561338595.
E-mail address: michel.chaussumier@isae.fr

doi:10.1016/j.proeng.2013.12.085

1. Introduction

Natural oxide layer formed at the surface of aluminium aeronautical parts is not thick enough to ensure a sufficient resistance of these parts in severe conditions and anodizing process is widely used in order to increase the wear resistance. However, this industrial process has deleterious consequences on resistance. Numerous researchers found important decrease of fatigue resistance for 2xxx and 7xxx aluminium alloys comparing to reference, often machined and polished surface state [1, 10]. Most of them explained the decrease by the porous nature and the brittle behavior of the oxide layer, and the tensile residual stresses at the interface between oxide layer and substrate; some others noticed the presence of pits defects at the surface as responsible for too.

Anodizisation is an electrolytic process that produced amorphous aluminium oxide at the surface [11]. This surface treatment includes a degreasing step followed by a pickling step and then the anodizing step. Usually, no surface deterioration can be observed after degreasing step. But during pickling process, according to aluminium alloy and pickling conditions, several pits can be produced due to the dissolution of intermetallic particles or aluminium matrix at the interface between intermetallic particles and matrix [12, 14]. Such results have been also observed by the author concerning chromic acid anodized 7010 aluminium alloy [15].

Experimental study on 7050 chromic acid anodized aluminium alloy is presented in this paper. Specimens, distributed in three groups (machined, machined and degreased, machined and pickled, machined and anodized), have been tested in four bending point fatigue test.

In order to predict fatigue life of this anodized alloy, an analytical model has been developed; it was based on Suraratchaï's model [16, 17] which has been developed at ICA-Toulouse on the principle of stress concentration effect generated by surface roughness resulting from machining. Applied to anodized surface, pits are considered as stress intensity concentrators which influence as well crack initiation and the beginning of crack propagation. In present paper, the analytical fatigue model is presented: new partial model concerning short fatigue crack initiation and propagation growth and oxide layer have been made comparing to previously presented model [15] which only concerned pickled surface state. In this model, local stress concentration coefficients induced by machining surface roughness and pickling pits are calculated using a 3D finite elements model built from experimental surface topographic measurements. Surface data are analyzed using a low pass filter in order to eliminate roughness profile details which are not relevant from fatigue failure mechanisms which have been identified from fractographic observations [17].

2. Experimentation

2.1. Material

Fatigue tests have been conducted on a 7050-T7651 aluminium alloy whose composition is given in Table I. Composition has been analyzed using EDS. Specimens provided from a laminate plate of 70 mm thickness. Microstructure was constituted with equiaxial recrystallized grain of mean size about 25-30 microns and highly elongated in the rolling direction unrecrystallized grains (figure 1). Al2CuMg, Al7Cu2Fe Mg2Si intermetallic particles have been detected mainly in recrystallized grains; the average size of these particles was about 8-12 micrometers.

Mechanical properties in the rolling direction are resumed in Table II.

Table I. EDS analyzed chemical composition of 7050 aluminium alloy.

Element	Average Content (wt%)	Element	Average Content (wt%)
Cu	1.76	Zn	6.15
Mg	2.42	Zr	0.14
Mn	0.07	Ti	0.06
Si	0.28	Al	Bal.
Fe	0.19		

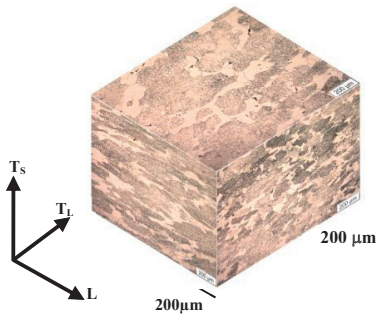

Figure 1. 3D microstructure of 7050-T7651 aluminium alloy
(L=Rolling direction, T-L=Transverse-long direction, TS=Transverse-short direction)

Table II. Mechanical properties of 7050 aluminium alloy in T-L direction.

Monotonic properties	Value	Paris' law coefficients	Value
Yield strength	440 MPa	Cfl	7.50 10-12
Ultimate strength	505 MPa	mfl	4.175
Elongation	11.4%	ΔKth	3.5 MPa√m
Young Modulus	72.6 GPa		

2.2. Fatigue test specimens

Fatigue test specimens were machined such as bending stress was applied in transverse-long direction. The geometry and the dimensions are given in figure 2. After milling, surfaces to be anodized were machined using a shaper HERMES-RS55 without any lubricant. Machining conditions have been chosen in order to obtain a surface roughness Ra of 0.8 micrometers; these conditions are given in Table III.

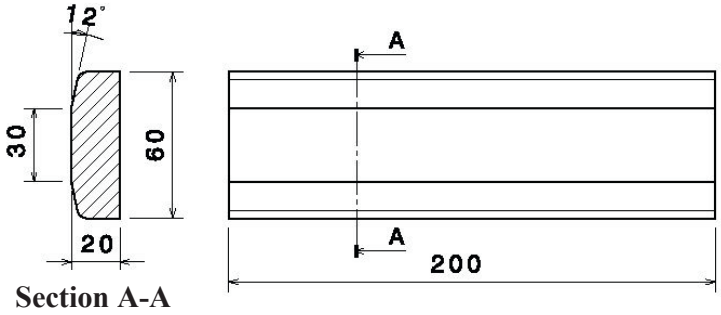

Figure 2. Fatigue test specimens geometry and dimensions (in mm)

Table III. Machining conditions.

Ra (µm)	cutting speed (m/mn)	feed (mm/cp)	depth of cut (mm)	tool nose radius (mm)
0.8	160	0.1	0.5	0.8

2.3. Surface treatments

Anodic oxidation has been realized in a chromic acid bath by our industrial partner in order to respect industrial protocols effectively used by industry. Before pickling process, specimens were degreased in order to produce a

chemical cleaned surface. This degreasing was carried out in alkaline solution (PH=9) at 60°C for 3 minutes followed by water rinsing. Pickling was done in two steps: a first one in a sodium solution at 32°C followed by rinsing and the second step in an ARDROX solution at 32°C for 3 minutes followed by rinsing. Chromic acid anodization was done in chromic CrO_3 solution at 40°C for 50 minutes in order to produce 3µm average thickness of oxide layer.

2.4. Fatigue tests

Specimens were tested in four-point bending fatigue on a 100 kN MTS servo-hydraulic fatigue machine at a frequency of 10 Hz at ambient temperature, under a stress ratio R of 0.1.Three groups of fatigue specimens have been created. The first one was constituted with only machined specimens; the second one with machined and pickled specimens; in the third one, specimens were machined, pickled and anodized. The first specimens group has been used to build a fatigue reference curve.

3. Experimentation

As surface was often responsible for fatigue crack initiation, surfaces were optically observed and topographic measurements have been systematically done in order to compare pickled and anodized surfaces with machined ones. It was observed that pickling process was highly deleterious for surface state: many pickling pits were observed resulting from dissolution of Al7Cu2Fe and Al2CuMg inter-metallic particles (figure 3a) during process. Concerning anodized surface, less pits could be observed as it can be seen on (figure 3b); this can be explained by the fact that previous pickling pits were recovered by the oxide layer if their size was small enough. On the contrary, pits size increased if their initial size was high enough. As it can be seen on figure 3b, width of smallest pits is about 7 micrometers; on the contrary, width of biggest pits could reach 50 microns along machined transverse direction.

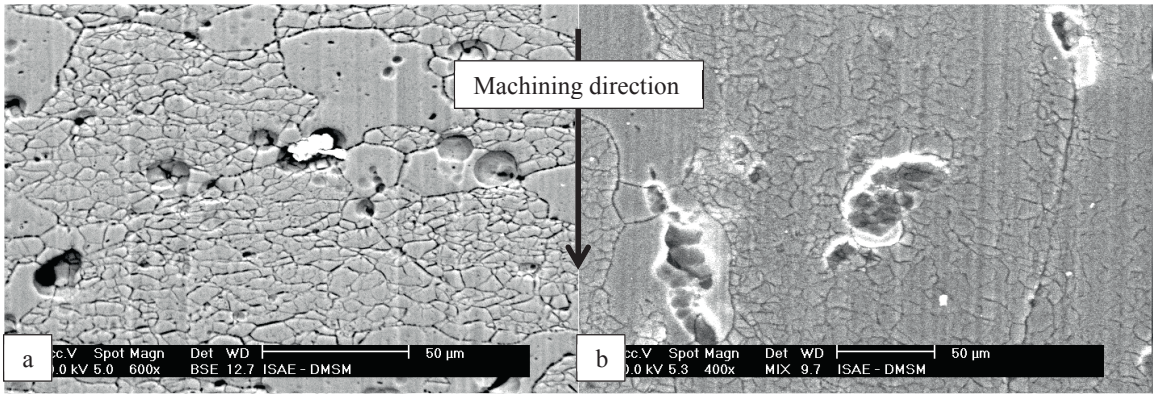

Figure 3. Influence of surface treatment on surface state – (a) after pickling – (b) after anodizing

As shown in figure 4, chromic acid anodizing led to an important decrease of fatigue resistance comparing to only machined specimens; There is no doubt that this decrease is due to the degradation of the surface during pickling process and then anodizing process. These effects are highly reduced as the stress level increases; this corresponds to the fact that, under high stress levels, influence of surface is less important and nucleation stage is considerably reduced comparing to propagation stage. SEM fractographic observations of each fractured specimens have been made in order to determine the failure mechanisms. In case of machined state, it has been observed that intermetallic particles Mg_2Si and Al_7Cu_2Fe were responsible for crack nucleation (figure 5). Generally, only one nucleation crack site could be observed except for high stress level where multi-cracks were observed. In case of pickled and anodized states, multiple nucleation sites have been observed whatever the stress level; the sites have been identified to the pickling pits (figure 6). Otherwise, coalescence of neighboring cracks has been equally observed.

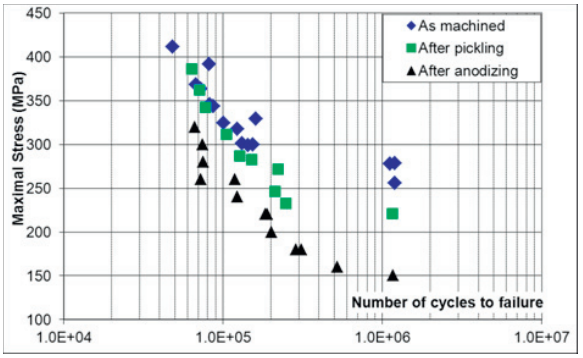

Figure 4. Four bending fatigue tests results for machined, pickled and anodized 7050 specimens

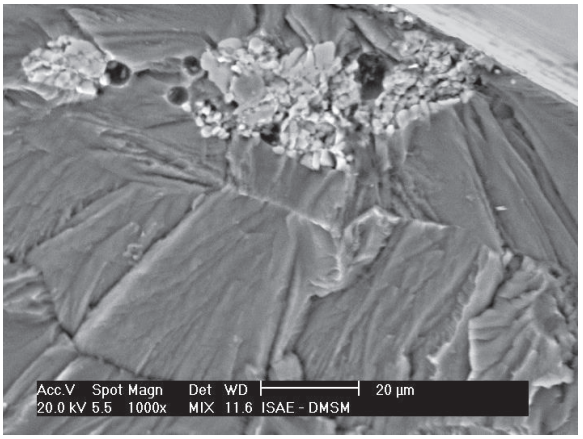

Figure 5. Crack nucleation from intermetallic particles Al7Cu2Fe for only machined specimens

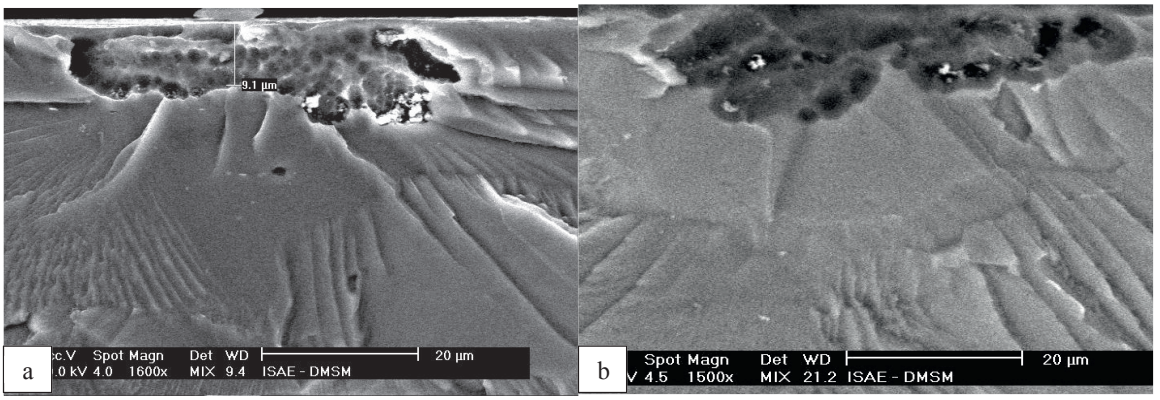

Figure 6. Crack nucleation from pickling pits (a) pickled specimens – (b) anodized specimens

4. Model

In order to take into account experimental observations conducted on pickled and anodized specimens, a fatigue life prediction model has been developed. It is built upon Suraratchaï's model [16] which is himself built upon the following consideration: fatigue cracks nucleate from the surface and nucleation is greatly influenced by metallurgy, residual stresses and geometry. From that point of view, Suraratchaï studied 7010 aluminium alloy and has shown that this material was largely more sensitive to geometry of the surface than to residual stress state or metallurgy [1]. . Later Shazhad studied 7050 aluminium alloy and reached the same conclusions [19- 21]. Such statement cannot be generalized to others kind or metallic alloys and experimental studies must be done to verify this relative sensitivity. Based on these experimental observations, Suraratchaï proposed a fatigue life model based on stress concentration coefficient induced by machining surface roughness [16] [22]. However, this model couldn't predict fatigue life in the case of anodized 7050 aluminium part: because the surface characterization through roughness profiles measurements was not able to give the real profile of pickling pits. In order to obtain more accuracy, surface topographic measurements have been used to build the finite element model from which local stress concentration coefficients are calculated. Otherwise, original Suraratchaï's model did not include the interaction between two neighboring cracks. This point has been integrated in the present model. Last, original model used traditional Paris's law for crack propagation calculation and does not take into account the micro crack stage: this point is presently considered.

The present model uses previous model [15] [23], which are resumed here:

- pickling pits are considered to be responsible for fatigue strength decrease as they act as stress concentrators which increase stress intensity factor range during the first stage of propagation;
- these defects are characterized (depth, length, width, shape) from topographic surface measurements and the surface repartition of these defects is characterized too;
- stress concentration coefficient at the location of pickling pits are calculated using a finite element model built from the experimental surface topography;
- fatigue life predictions are done considering the all set of defects; propagation is calculated simultaneously for each crack; the used crack propagation law introduces a short crack stage propagation law and naturally Paris' law is used when cracks are long enough to be considered as long cracks; a coalescence criteria if also introduced to consider possible interaction between neighboring cracks.

These several principles are more detailed in the following sections.

4.1. Surface characterization

Cracks propagation rate depends on stress intensity factor range which depends on crack length. In case of pickled and anodized 7050 aluminium parts, as fatigue cracks nucleate from pickling pits, accurate calculations needs accurate shape characterization. In present study, shapes and positions of pickling pits have been characterized using a Mahr PKG120 profilometer with a conical diamond stylus (60°- 2 micrometers radius). Several specimens of surfaces of 0,5x2 mm² have been measured on each fatigue test specimens in order to conduct statistical calculations. Mean size pickling pits has been estimated to 4.78 micrometers.

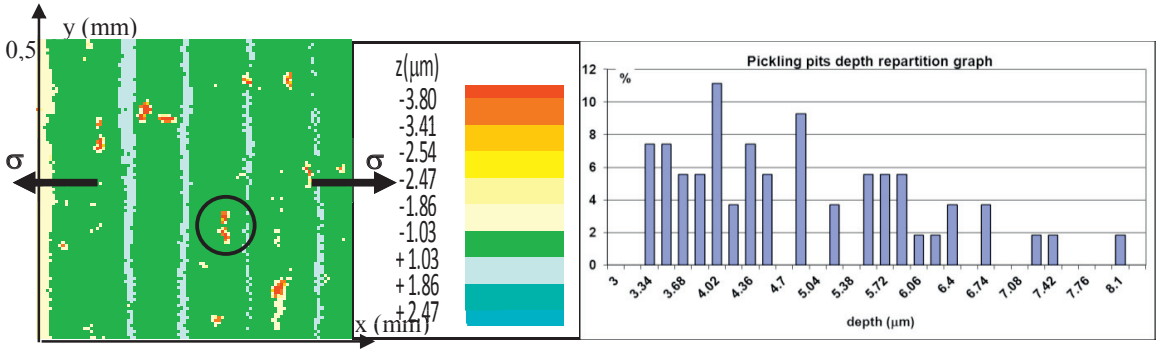

Figure 7. Example of surface characterization and depth repartition graph for pickling condition

4.2. Stress concentration coefficient calculation

Stress concentration coefficient induced by machining roughness and pickling pits were conducted using a 3D finite elements model of a representative elementary volume. Surfaces (0.5x0.5 mm²) of this volume were built from surface topography measurements. The surface refined mesh is chosen from the resolution used for surface topography, i.e. 5x5x5 micrometers. The calculations were conducted using elastic hypothesis; displacements were applied along x direction, perpendicular to machining direction.

Local stress $\sigma_{i,loc}^{\max}$ used in local stress concentration coefficient Kt_i definition was calculated using an average on five elements depth: that corresponds to the average size of grains in which pits were detected.

$$Kt_i = \frac{\sigma_{i,loc}^{\max}}{\sigma_{nom}^{\max}} \tag{1}$$

4.3. Crack propagation model

Pickling pits are considered as initial flaws from which micro-cracks could nucleate if stress intensity factor is high enough. At this scale, where crack size is largely less than grain size, long crack theory could not be used [24]. Consequently, a short crack law was introduced. If mechanisms of propagation of short cracks are better known, few models are available [25-27]. In a previous model [23], a simple short crack propagation law has been proposed. In the present model, the short crack propagation law is based on Santus and Taylor model [27]

As well as long crack threshold, short crack threshold depends on material microstructure and stress ratio; for each pit, of initial depth a_i, the short crack threshold has been evaluated using El Haddad short crack threshold equation [**Erreur ! Source du renvoi introuvable.**]:

$$\Delta K_{th,a_i} = \Delta K_{th} \cdot \sqrt{\frac{a_i}{a_i + \frac{a_0}{\beta^2}}} \tag{2}$$

were ΔK_{th} represents the long crack threshold defined for the same stress ratio as used for the fatigue test, β is the geometric factor and a_0 is the length of the longest crack which does not propagate under fatigue limit stress range $\Delta\sigma_D$:

$$a_0 = \frac{1}{\pi} \cdot \left(\frac{\Delta K_{th}}{\Delta \sigma_D} \right)^2 \quad (3)$$

According to Santus' model [27], the short crack propagation law is based on Zheng and Hirt model, introducingan effective stress intensity factor range:

$$\left. \frac{da}{dN} \right|_{fc} = C_{fc} \cdot \Delta K_{eff}^{\ m_{fc}} \quad (4)$$

$$with\ \Delta K_{eff} = \Delta K_{sc} - \Delta K_{th_{sc}} \quad (5)$$

where ΔK_{SC} represents the stress intensity range factor for a short crack and $\Delta K_{th_{sc}}$ the short crack threshold as defined by equation (2).

In equation (3), C_{sc} and m_{sc} represent the coefficients of the short crack propagation law. Let remark that, among the several models available in the literature, Santus' choice of Zhen and Hirt model is based only the simplicity of the model and the quality of fitting of the smooth transition at the near threshold conditions, even if mechanistic justifications could be discussed.

As no experimental data were available, some assumptions have been made concerning micro-crack propagation rate law: the coefficients C_{sc} and m_{sc} have been chosen accordingly with experimental data concerning 7075-T6 aluminium alloy: the ratio between C_{sc} - C_{lc} and m_{sc} - m_{lc} have been found to be 0.5 and 200 respectively.

4.4. Cracks are considered to be semi-elliptical cracks; in the expression of stress intensity factor range, whatever was the crack stage, geometric factors at the bottom of the semi-elliptical crack and at the surface tip of the crack have been calculated using Newman-Raju model [29].Stress concentration at pit locations

It has been shown experimentally that surface roughness was the principal influence factor in fatigue behavior of present 7050 alloy. In case of anodized specimens, this effect was reinforced by the presence of numerous pickling pits who acted as microcrack nucleators. Under loading, these pits were subjected to higher stress levels which depend on pit size. In the present model, this has been taken into account through the stress concentration factor magnification of the stress range during propagation through the depth. Otherwise, for through depth propagation, it was assumed that this stress concentration effect was effective as long as the crack could be considered as a short crack, i.e., until crack growth rate reached long crack growth rate. This assumption is expressed with the following relations:

$$\Delta K_{a_i} = \alpha_{0^\circ} \cdot Kt_{a_i} \cdot \Delta \sigma \cdot \sqrt{\pi a_i} \quad while\ \Delta K_{a_i} \le \Delta K_{Tr_{sc/lc}} \quad (6)$$

$$\Delta K_{a_i} = \alpha_{0^\circ} \cdot \Delta \sigma \cdot \sqrt{\pi a_i} \quad while\ \Delta K_{a_i} \le \Delta K_{Tr_{sc/lc}} \quad (7)$$

For surface propagation, surface roughness influence was always considered so that it came:

$$\Delta K_{c_i} = \alpha_{90^\circ} \cdot Kt_{surf} \cdot \Delta \sigma \cdot \sqrt{\pi c_i} \quad (8)$$

In the above relations, $\propto_{0°}$ and $\propto_{90°}$ represents the geometric factor, respectively at the bottom and the surface of pits, assuming that pit shape could be considered as semi-elliptical flaws.

4.5. Coalescence condition during cracks propagation

It was assumed that two neighboring cracks could coalesce if they were close enough so that the plastic zone which developed at crack tips could reach [30]. This condition has been introduced in the present model using the following relation:

$$d_{ij} \leq zp_i + zp_j \tag{9}$$

where d_{ij} represent the shorter distance between the crack tips of two neighboring crack i and j, z_{pi} and z_{pj} the plastic areas diameter of these two cracks

When this condition, which is controlled at each calculation step, is respected, a new crack is considered which covered the two previous cracks.

4.6. Anodized surface model

It has been observed that the number of discernible pits decrease after anodizing: the smallest pits were covered by oxide layer. So it was more difficult to have an accurate characterization of the surface topography of anodized specimens. Simultaneously, SEM observations showed that size of the biggest pickling pits increased. In present model, anodized surface topography is deduced from pickled surface topography, using a post-treatment of topography measurements: if depth of one pickling pit was smaller than a threshold, defined from surface observations, then size was unchanged; on the contrary, size of pit was increased. The threshold has been chosen equal to the depth corresponding to the width of the smaller measured pit, assuming a shape ratio c/a of 1. The level of size increase over this threshold has been calculated accordingly to the empirical pit growth relation:

$$r = k \cdot t^m \tag{10}$$

where *k* and *m* represent a material specific constant to be determined with experiments [31].

For present anodizing treatment conditions (50 minutes at 40°C), the increase of size is estimated to 2.5 microns. As no pits whose width was less than about 7 microns, it can be deduced that all pits smallest than 4 microns was recovered by the oxide layer and depth threshold have been chosen equal to 4 microns. Let's remark that this value corresponded to mean depth of characterized pickling pits (4.8 micrometers).

5. Simulations results and discussion

The following figures show examples of FE analysis results and stress concentration coefficient repartition graphs given by finite elements simulations for as machined (figure 8) and pickled state (figure 9). As is can be seen, compared to machining surface roughness influence, characterized with a mean stress concentration coefficient of 1.186, presence of pickling pits degrades considerably surface: mean stress concentration increase of 45%. As in case of 7050-T6, previous studies have shown that, among the three parameters which can influence fatigue behavior, surface roughness was the most influent, it can be obviously deduced that the experimentally observed decrease of fatigue resistance for anodized specimens can be attributed to the surface degradation. However, the fatigue resistance decrease experimentally observed (20%) cannot be directly linked to the increase of mean value of the stress concentration coefficient as it would be equivalent to consider a single initial defect: that does not reflect the experimental observations (multi-cracking).

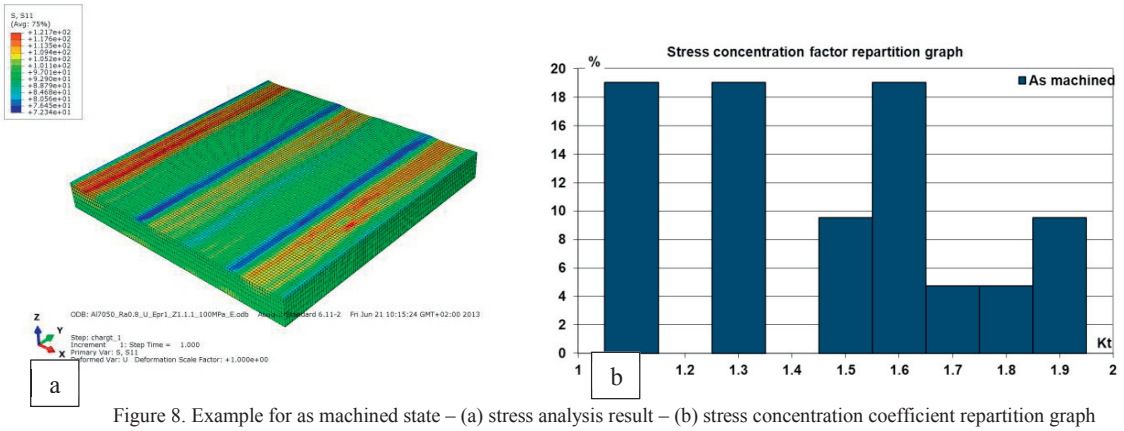

Figure 8. Example for as machined state – (a) stress analysis result – (b) stress concentration coefficient repartition graph

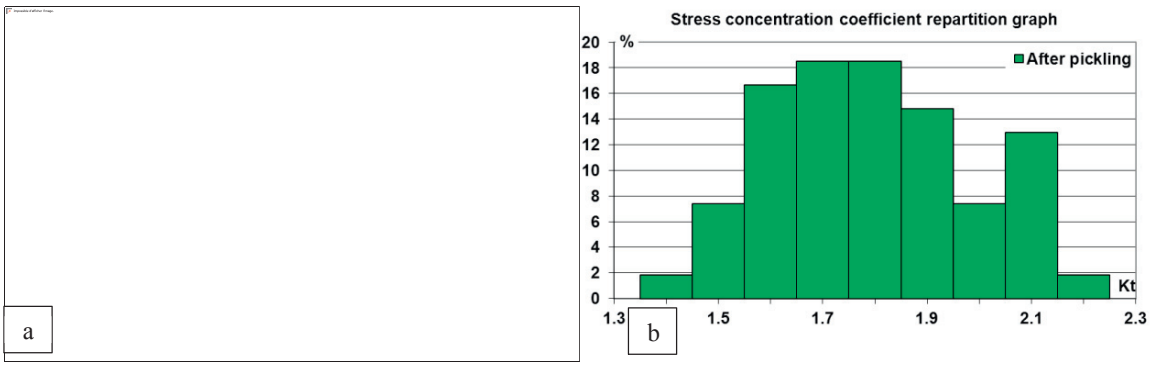

Figure 9. Example for pickled state – (a) stress analysis result – (b) stress concentration coefficient repartition graph

The following figures show the results obtained with the presented fatigue life prediction model for the three different surface states: as machined state (figure 10), pickled state (figure 11) and anodized state (figure 12). The presented results correspond to few specimens; no statistical study has been made yet but it is assumed that the chosen specimens were representative of the different surface states. As one can see, previsions are in very good agreement with experimental data for the three surface states.

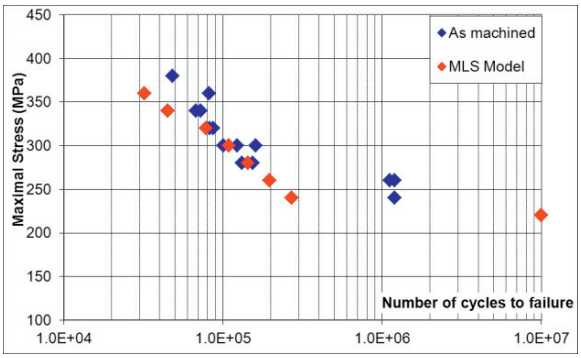

Figure 10. Predictions versus experimental number of cycles to failure for as machined state (example)

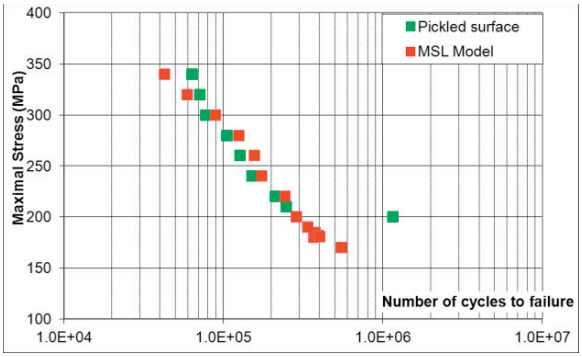

Figure 11. Predictions versus experimental number of cycles to failure for pickled state (example)

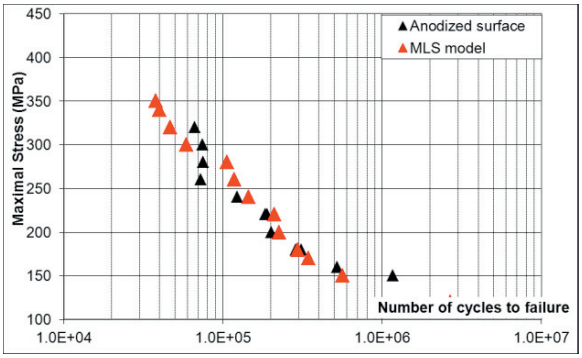

Figure 12. Predictions versus experimental number of cycles to failure for anodized state (example)

6. Conclusion

Four point bending fatigue tests under stress ratio R0.1 have been realized on 7050-T6 as machined, pickled and chromic acid anodized specimens in order to precise the influence of each process step from machining to anodizing. An important decrease of fatigue resistance has been observed for anodized specimens; more than half of this decrease can be attributed to pickling process which leads to sever pitting of the surface. Pits were found to result from dissolution of intermetallic particles or dissolution of the aluminium matrix at the interface matrix/particles. It has been observed smaller pickling pits were recovered by oxide layer while size of severe pits increased during anodizing process. Crack nucleation sites have been identified: for as machined state, fatigue cracks nucleate from intermetallic particles near the surface; for pickled and anodized states, cracks nucleate from pits where previously, intermetallic particles were.

In order to make fatigue life predictions for chromic acid anodized 7050 aluminium parts, a model has been developed based on local Kt approach. 3D finite elements models were built from surface topography measurements. A short crack stage was considered in the model including a short crack stress intensity threshold and a short crack growth rate law. Short crack stress intensity threshold was calculated using El Haddad' model ; the short crack propagation law was based on Santu's model and relations between long crack growth rate parameters (Paris' law) and short crack growth rate parameters deduced from 7075 aluminium alloy data.

For each as machined and pickled state, pits are identified by a scanning process using a contact perthometer; as surface topography measurements of anodized surface were not representative because most of little pickling pits were covered by oxide layer, useful surfaces for FE models were deduced from measured pickled surfaces and size of major pickling pits were increased using a corrosion power law; oxide layer was considered through an artificial increase of initial short crack.

Calculations have been done simultaneously for each pits identified during scanning process and coalescence condition between neighboring cracks has been verified at each calculation step. Predictions are found to fit experimental data with very good agreement considering the assumptions which have been made.

Acknowledgements

The authors acknowledge the experimental support from AIRBUS France – Toulouse.

References

[1] Cree A.M., Weidmann G.W., Effect of anodized coatings on fatigue cracks rates of aluminium alloy*, Surface Engineering*, 13 (1), 1997, 51-55

[2] Pao P.S., Gill S.J. Feng C.R., On fatigue crack initiation from corrosion pits in 7075-T7351 aluminium alloy, *Scripta Materialia*, 43 (5), 1998, 391-396.

[3] Rokhlin S.I., Kim J.Y., Nagy H., Zoofan B., Effect of pitting on fatigue crack initiation and fatigue life, *Engineering Fracture Mechanics*, 62, 1998, 425-44

[4] Dolley E.J., Wei R.P., The effect of pitting corrosion on fatigue life, *Fatigue and Fracture of Engineering Materials and Structures*, 23, 2000, 555-560.

[5] Kermanidis AL. Th., Petroyiannis P.V., Pantelakis S. G., Fatigue damage tolerance behaviour of coroded 2024 T351 aircraft aluminium alloy, *Theorical and Applied Fracture Mechanics*, 43, 2005 121-132

[6] Rateick R. G., Griffith R. J., Hall D. A., Thompson K. A., Relationship of microstructure to fatigue strength loss in anodized aluminium-copper alloys*, Materials Science and Technology*, 21, 2005, 1227-1235.

[7] Sadeler R., Effect of a commercial hard anodizing on the property of a 2024-T6 aluminium alloy, *Journal of Materials Science*, 41, 2006, 5803-5809

[8] Lonyuk B., Apachitei I, Duszczyk J., The effect of oxide coatings on fatigue properties of 7475-T6 aluminium alloy, *Surface and Coatings Technology*, 201 (21), 2007, 8688-8694

[9] Camargo A., Voorwald , Influence of anodization on the fatigue strength of 7050-T7451 aluminium alloy, *Fatigue Fracture of Engineering Materials & Structures*, 30, 2007, 993-1007

[10] Cyrik E., Genel K., Effect of anodic oxidation on the fatigue performance of 7075-T6 alloy, *Surface and Coatings Technology*, 202, 2008, 5190-5201

[11] ASM Handbook, Corrosion, vol. 13, ASM International, USA, 1992.

[12] Thompson G. E., Zhang L., C. Smith J. E., Skeldon P., Boric/sulfuric acid anodizing of aluminum alloys 2024 and 7075: Film growth and corrosion resistance, *Corrosion Science*, 55, 1999, 1052-1060.

[13] Snogan F., Blanc C., Mankowski G., Pébère N., Characterisation of sealed anodic films on 7050 T74 and 2214 T6 aluminium alloys, *Surface and Coatings Technology*, 154, 2002, 94-103.

[14] Liu, J.H. Li M., Li S. M., Huang M., Effect of the microstructure of Al 7050-T7451 on anodic oxide formation in sulfuric acid, *International Journal of Mineral*, *Metallurgy and Materials*, 16, 2009, 432-438.

[15] Chaussumier M., Shahzad M., Mabru C., Chieragatti R., Rezaï-Aria F., A fatigue multi-site cracks model using coalescence, short and long crack growth laws, for anodized aluminum alloys, *Procedia Engineering*, 2 (1), 2010, 995-1004

[16] Suraratchaï M., Limido J., Mabru C., Chieragatti R., Modelling the influence of machined surface roughness on the fatigue life of aluminium alloy, *International Journal of Fatigue*, 30 (12), 2008, 2119-2126.

[17] Chieragatti R., Espinosa C., Lacome J.H., Limido J., Mabru C., SALAUN M., Influence of roughness on the fatigue of machined surfaces: determination of local stress concentration *,* 29èmes journées de Printemps, JP 2010, 2010, 19-20

[1] Suraratchaï M., Influence de l'état de surface sur la tenue en fatigue de l'alliage d'aluminium 7010, PhD thesis, Université de Toulouse III, France, 2006

[19] Shahzad M, Influence de l'usinage et de l'anodisation sur le comportement en fatigue d'alliages d'aluminium aéronautiques, PhD thesis, Université de Toulouse, 2010

[20] Shahzad M., Chaussumier M., Chieragatti R., Mabru C, Rezaï-Aria F., Influence of surface treatments on fatigue life of Al 7010 alloy, *Journal of Materials Processing Technology*, 210 (13), 2010, 1821-1826.

April 2010, pp 1015-1024

[21] Shahzad M., Chaussumier M., Chieragatti R., Mabru C., Rézaï-Aria F., Surface characterization and influence of anodizing process on fatigue life of 7050 alloy*, Materials and Design*, 32 (6), 2011, 3328-3335.

[22] Chieragatti R, Surarachai M, Mabru C, Espinosa C, Vergnes V., Procédés de caractérisation de la tenue en fatigue d'une pièce à partir de son profil de surface, French Patent n°0650793, 2006.

[23] Chaussumier M., Mabru C., Shahzad M., Chieragatti R., Réza¨-Aria F., A predictive fatigue life model for anodized aluminium alloy, International Journal of Fatigue, 48, 2013, 205-213.

[24] Pearson S., Initiation fatigue cracks in commercial aluminium alloys and the subsequent propagation of very short cracks, *Engineering Fracture Mechanics*, 7 (2), 1975, 235-247

[25] Newman J.C., Philipps E.P., Swain M.H., Fatigue life prediction methodology using small-crack theory, *International Journal of fatigue*, 21, 1999, 109-119.

[25] Chapetti M.D., Fatigue propagation threshold of short cracks under constant amplitude loading, *International Journal of Fatigue*, 25, 2003, 1319-1326.

[27] Santus C., Taylor D., Physically short crack propagation in metals during high cycle fatigue, *International Journal of Fatigue*, 31, 2009, 1356-1365.

[**Erreur ! Source du renvoi introuvable.**] El Haddad M.H., Topper T.H., Smith K.N, Prediction of non propagating cracks, *Engineering Fracture Mechanics*, 11 (3), 1979, 573-584.

[29] Newman J.C., Raju I.S., Stress-intensity factor equations for cracks in three dimensional finite bodies subjected to tension and bending loads, *Computational Methods in Mechanics of Fracture*, pp. 312-334, Ed ATLURI S.N., Elsevier Science Publishers,1986.

[30] DeBartolo E.A. , Hillberry B.M., A model of initial flaw sizes in aluminium alloys, *International Journal of Fatigue*, *International Journal of Fatigue*, 23, 2001, 79-86.

[31] Cabrol S., Modélisation de la croissance des piqures dans l'alliage d'aluminium 2024 T351 en milieu chloruré, *Ann. Chim.* Sci. Mat., 24, 1999, 307-311